



Curvilinear crosscuts of subdivision for a domain decomposition method in numerical conformal mapping

M.I. Falcão^a, N. Papamichael^b, N.S. Stylianopoulos^{b,*}

^aCentro de Matemática, Universidade do Minho, Campus de Gualtar, 4700 Braga, Portugal

^bDepartment of Mathematics and Statistics, University of Cyprus, P.O. Box 20537, Nicosia, Cyprus

Received 5 November 1998; revised 1 February 1999

Abstract

Let $Q := \{\Omega; z_1, z_2, z_3, z_4\}$ be a quadrilateral consisting of a Jordan domain Ω and four points z_1, z_2, z_3, z_4 in counterclockwise order on $\partial\Omega$. We consider a domain decomposition method for computing approximations to the conformal module $m(Q)$ of Q in cases where Q is 'long' or, equivalently, $m(Q)$ is 'large'. This method is based on decomposing the original quadrilateral Q into two or more component quadrilaterals Q_1, Q_2, \dots and then approximating $m(Q)$ by the sum $\sum_j m(Q_j)$ of the modules of the component quadrilaterals. The purpose of this paper is to consider ways for determining appropriate crosscuts of subdivision (so that the sum $\sum_j m(Q_j)$ does indeed give a good approximation to $m(Q)$) and, in particular, to show that there are cases where the use of curved crosscuts is much more appropriate than the straight line crosscuts that have been used so far. © 1999 Elsevier Science B.V. All rights reserved.

MSC: 30C30; 65E05

Keywords: Numerical conformal mapping; Quadrilateral; Conformal module; Domain decomposition

1. Introduction

Let $Q := \{\Omega; z_1, z_2, z_3, z_4\}$ be a quadrilateral consisting of a Jordan domain Ω and four points z_1, z_2, z_3, z_4 in counterclockwise order on $\partial\Omega$ and let $m(Q)$ be the conformal module of Q . Also, let $R_{m(Q)}$ denote a rectangle of base $m(Q)$ and height 1, i.e.

$$R_{m(Q)} := \{w: 0 < \Re w < m(Q), 0 < \Im w < 1\}.$$

Then, Q is conformally equivalent to the rectangular quadrilateral

$$\{R_{m(Q)}; i, 0, m(Q), m(Q) + i\},$$

* Corresponding author.

E-mail addresses: mif@math.uminho.pt (M.I. Falcão), nickp@ucy.ac.cy (N. Papamichael), nikos@ucy.ac.cy (N.S. Stylianopoulos)

in the sense that there exists a unique conformal map $f: \Omega \rightarrow R_{m(Q)}$ that takes the four points z_1, z_2, z_3, z_4 , respectively, onto the four vertices $i, 0, m(Q), m(Q) + i$ of $R_{m(Q)}$.

This paper is concerned with the study of a domain decomposition method (DDM) for computing the conformal modules of long quadrilaterals. The DDM was introduced by two of the present authors (N.P. and N.S.S.) in [10,11], for the purpose of computing the conformal modules and associated conformal maps of a special class of quadrilaterals. The method was also studied by the same authors in [12–15] and by Gaier and Hayman [3,4], in connection with the computation of conformal modules, and by Laugesen [8] in connection with the determination of the associated conformal maps. For the computation of conformal modules, the method consists of the following two main steps:

- (i) Decomposing the original quadrilateral Q (by means of appropriate crosscuts $l_j, j = 1, 2, \dots$) into two or more component quadrilaterals $Q_j, j = 1, 2, \dots$
- (ii) Approximating the conformal module $m(Q)$, of the original quadrilateral, by the sum $\sum_j m(Q_j)$ of the conformal modules of the component quadrilaterals.

(Note that

$$m(Q) \geq \sum_j m(Q_j) \tag{1.1}$$

and equality occurs only when the images of all the crosscuts l_j under the conformal map $f: \Omega \rightarrow R_{m(Q)}$ are straight lines parallel to the imaginary axis. This follows from the well-known composition law for modules of curve families; see e.g. [1, pp. 54–56] and [5, pp. 437–438].)

The problem of determining $m(Q)$ is closely related with that of measuring resistance values of electrical networks and, in this connection, the DDM is of considerable practical interest for the following two reasons:

- (i) It can be used to overcome the crowding difficulties associated with the problem of computing the modules of long quadrilaterals, i.e. the difficulties associated with the conventional approach of seeking to determine $m(Q)$ by first mapping Ω onto the unit disc or the half plane (see e.g. [9, Section 3.1] and [13, Section 1]).
- (ii) It takes advantage of the fact that in many applications (for example VLSI applications) a complicated original quadrilateral Q can be decomposed into very simple components Q_j (see e.g. [14,15]).

Our work in this paper is concerned with the fact that all the available DDM theory is based on the use of straight line crosscuts of subdivision. Our specific objective here is to investigate whether there are cases for which the use of curved crosscuts is more appropriate. In this context, we describe a simple technique for determining curved crosscuts of decomposition and show, by means of examples, that there are many cases for which the use of such crosscuts is more appropriate than the straight lines that have been used so far.

In presenting our results we shall adopt throughout the notations used in [12–14]. That is:

- Ω and $Q := \{\Omega; z_1, z_2, z_3, z_4\}$ will denote respectively the original domain and corresponding quadrilateral.

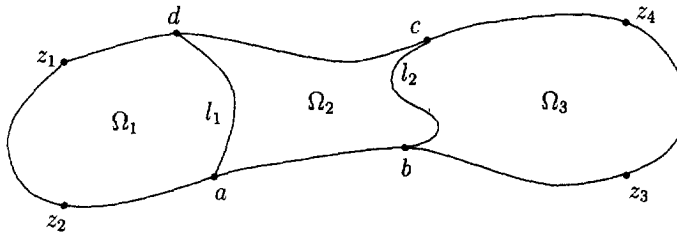


Fig. 1.

- $\Omega_1, \Omega_2, \dots$, and Q_1, Q_2, \dots , will denote, respectively, the ‘principal’ sub-domains and corresponding quadrilaterals of the decomposition under consideration.
- The additional subdomains and associated quadrilaterals that arise when the decomposition of Q involves more than one crosscut will be denoted by using (in an obvious manner) a multisubscript notation.

For example, the five component quadrilaterals of the decomposition illustrated in Fig. 1 are

$$Q_1 := \{\Omega_1; z_1, z_2, a, d\}, \quad Q_2 := \{\Omega_2; d, a, b, c\}, \quad Q_3 := \{\Omega_3; c, b, z_3, z_4\},$$

$$Q_{1,2} := \{\Omega_{1,2}; z_1, z_2, b, c\}, \quad Q_{2,3} := \{\Omega_{2,3}; d, a, z_3, z_4\},$$

where

$$\bar{\Omega}_{1,2} := \bar{\Omega}_1 \cup \bar{\Omega}_2, \quad \bar{\Omega}_{2,3} := \bar{\Omega}_2 \cup \bar{\Omega}_3.$$

2. A method for determining curved crosscuts

The available DDM theory for conformal modules, given in [12–15] and, in particular, the results of Theorems 2.4 and 2.6 of [15] can be used to derive approximations of remarkable accuracy to the modules of very complicated quadrilaterals of the type that occur frequently in VLSI applications (see the numerical examples given in [12–15]). These results, however, suffer from the following two drawbacks: (a) they require that the quadrilateral under consideration involves substantial symmetry (see e.g. the requirements of Theorems 2.4 and 2.6 of [15]); (b) they allow only for straight line crosscuts, although there are situations where, intuitively speaking, curved crosscuts appear to be much more appropriate.

The purpose of this section is to describe a simple, and yet very effective, device for overcoming the above drawbacks, in cases where the quadrilateral $Q := \{\Omega; z_1, z_2, z_3, z_4\}$ is characterised by the following (see Fig. 2) :

- (i) The defining domain Ω is part of an infinite polygon \mathcal{P} .
- (ii) $\partial\Omega$ consists of two segments of the opposite components of $\partial\mathcal{P}$ and two Jordan arcs γ_1 and γ_2 each joining the two opposite components of $\partial\mathcal{P}$.
- (iii) The points z_1, z_2 and z_3, z_4 of Q are points on the boundary arcs γ_1 and γ_2 , respectively.
- (iv) There is a corner point $b \in \partial\Omega \cap \partial\mathcal{P}$ through which it is, in some sense, ‘natural’ to seek to determine a crosscut l , thus decomposing Q into two ‘simpler’ component quadrilaterals

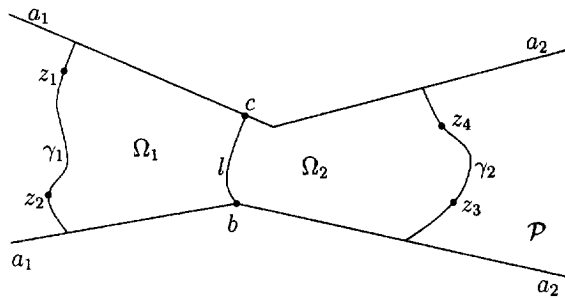


Fig. 2.

$Q_1 := \{\Omega_1; z_1, z_2, b, c\}$ and $Q_2 := \{\Omega_2; c, b, z_3, z_4\}$. (Of course, the crosscut l must be determined so that the sum $m(Q_1) + m(Q_2)$ is a good approximation to $m(Q)$.)

With reference to Fig. 2, let T be the Schwarz–Christoffel transformation that maps the upper half plane \mathcal{H} onto the infinite polygon \mathcal{P} so that

$$T(0) = a_1, \quad T(1) = b, \quad \text{and} \quad T(\infty) = a_2,$$

where a_1 and a_2 denote the two vertices of \mathcal{P} at infinity. Then, we claim that an appropriate crosscut l for the subdivision of the quadrilateral $Q := \{\Omega; z_1, z_2, z_3, z_4\}$ is given in parametric form by

$$l := \{z: z = T(e^{i\pi t}), 0 \leq t \leq 1\}. \tag{2.1}$$

The above choice of l can be justified as follows:

Let \mathcal{S} denote the infinite strip

$$\mathcal{S} := \{w = s + it: 0 < t < 1\}.$$

Then, the transformation

$$\Phi: w \rightarrow T(e^{\pi w}), \tag{2.2}$$

maps \mathcal{S} onto \mathcal{P} so that $\Phi(0) = b$ (see Fig. 3). This shows that the crosscut l of (2.1) is, in fact, the image under the conformal map $\Phi: \mathcal{S} \rightarrow \mathcal{P}$ of the straight line λ joining the points 0 and i on $\partial\mathcal{S}$, i.e. $l = \Phi(\lambda)$.

Let $Q := \{\Omega; z_1, z_2, z_3, z_4\}$ be a quadrilateral of the form illustrated in Fig. 2 and assume that the four points z_1, z_2, z_3, z_4 , are the four end points of the arcs γ_1 and γ_2 , i.e. the four corners where γ_1 and γ_2 meet $\partial\mathcal{P}$ (see Fig. 4(a)). Further, let $\hat{Q} := \{\hat{\Omega}; w_1, w_2, w_3, w_4\}$ denote the image of $Q := \{\Omega; z_1, z_2, z_3, z_4\}$, under the transformation $\Phi^{[-1]}: \mathcal{P} \rightarrow \mathcal{S}$, and let $\hat{\Omega}_1$ and $\hat{\Omega}_2$ denote respectively the corresponding images of the subdomains Ω_1 and Ω_2 (see Fig. 4(b)). Then, we have the following:

Theorem 2.1. For the decomposition illustrated in Fig. 4(a)

$$0 \leq m(Q) - \{m(Q_1) + m(Q_2)\} \leq 5.33e^{-2\pi m^*}, \tag{2.3}$$

provided that $m^* := \min\{m(Q_1), m(Q_2)\} \geq 1$.

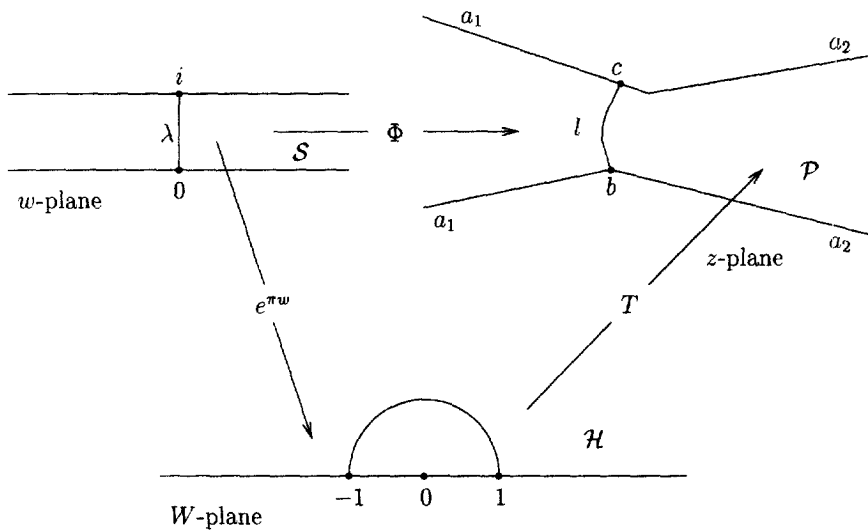


Fig. 3.

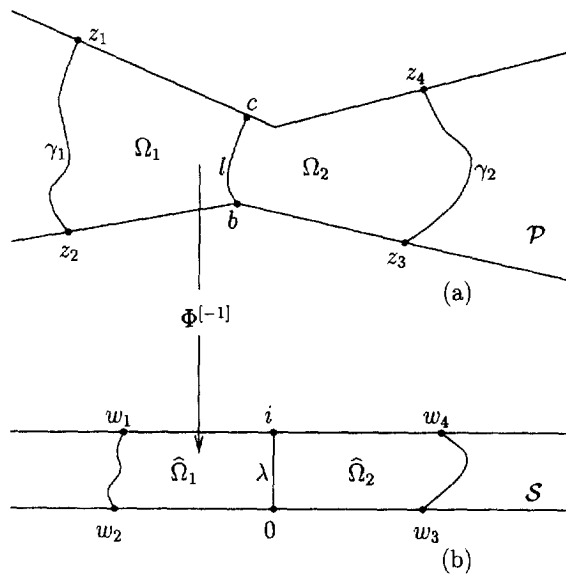


Fig. 4.

Proof. The result follows by applying Theorem 2.2 of [15] to the decomposition of the transformed quadrilateral \hat{Q} illustrated in Fig. 4(b) and recalling that conformal modules are conformally invariant. \square

We consider now the more general case, where the two points z_3, z_4 of the quadrilateral $Q := \{\Omega; z_1, z_2, z_3, z_4\}$ are not necessarily the two end points of γ_2 . In this case, for the statement and proof of the

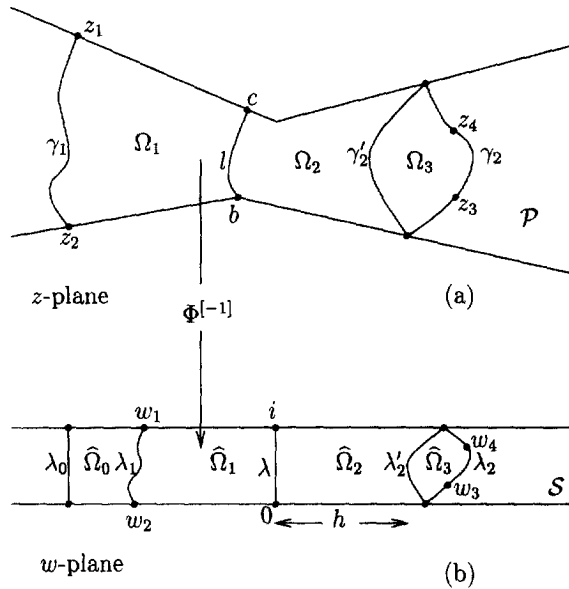


Fig. 5.

corresponding decomposition result, it is convenient to introduce an auxiliary crosscut γ'_2 , as shown in Fig. 5(a). That is, γ'_2 is a Jordan arc in Ω that shares the same end points with γ_2 and, together with the crosscut l , divides Ω into three subdomains Ω_1, Ω_2 and Ω_3 , so that $\bar{\Omega} = \bar{\Omega}_1 \cup \bar{\Omega}_2 \cup \bar{\Omega}_3$. Further, we let $\hat{Q} := \{\hat{\Omega}; w_1, w_2, w_3, w_4\}$, $\hat{\Omega}_1, \hat{\Omega}_2, \hat{\Omega}_3, \lambda_1, \lambda_2$ and λ'_2 denote, respectively, the images of $Q := \{\Omega; z_1, z_2, z_3, z_4\}$, $\Omega_1, \Omega_2, \Omega_3, \gamma_1, \gamma_2$ and γ'_2 , under the transformation $\Phi^{-1} : \mathcal{P} \rightarrow \mathcal{S}$ (see Fig. 5(b)).

Theorem 2.2. *Let Q be the quadrilateral of Fig. 5(a) described above. Then, for the decomposition defined by the curved crosscut l ,*

$$0 \leq m(Q) - \{m(Q_1) + m(Q_{2,3})\} \leq 28.52e^{-2\pi m^*}, \tag{2.4}$$

provided that $m^* := \min\{m(Q_1), m(Q_2)\} \geq 1.5$.

Proof. With reference to Fig. 5(b), let λ_0 be a straight line to the left of the arc λ_1 , parallel to λ and joining the lines $\Im w = 0$ and $\Im w = 1$, and denote by $\hat{\Omega}_0$ the domain bounded by the straight lines $\Im w = 1, \lambda_0, \Im w = 0$ and the arc λ_1 . Also, let $\hat{Q}_{0,1}, \hat{Q}_{0,1,2}$ and $\hat{Q}_{0,1,2,3}$ denote, respectively, the three quadrilaterals defined by the domains $\hat{\Omega}_{0,1}, \hat{\Omega}_{0,1,2}$ and $\hat{\Omega}_{0,1,2,3}$, where

$$\overline{\hat{\Omega}_{0,1}} = \overline{\hat{\Omega}_0} \cup \overline{\hat{\Omega}_1}, \quad \overline{\hat{\Omega}_{0,1,2}} = \overline{\hat{\Omega}_{0,1}} \cup \overline{\hat{\Omega}_2} \quad \text{and} \quad \overline{\hat{\Omega}_{0,1,2,3}} = \overline{\hat{\Omega}_{0,1,2}} \cup \overline{\hat{\Omega}_3}.$$

Then, by applying Theorems 2.5 and 2.2 of [15] to the quadrilaterals $\hat{Q}_{0,1,2,3}$ and $\hat{Q}_{1,2}$ respectively, we find that

$$|m(\hat{Q}_{0,1,2,3}) - \{m(\hat{Q}_{0,1,2}) + m(\hat{Q}) - m(\hat{Q}_{1,2})\}| \leq 2.71 e^{-\pi m(\hat{Q}_{1,2})}, \tag{2.5}$$

provided $m(\hat{Q}_{1,2}) \geq 3$, and

$$0 \leq m(\hat{Q}_{1,2}) - \{m(\hat{Q}_1) + m(\hat{Q}_2)\} \leq 5.33 e^{-2\pi m^*}, \tag{2.6}$$

provided $m^* := \min\{m(\hat{Q}_1), m(\hat{Q}_2)\} \geq 1$. Also, if h denotes the distance of the straight line λ from the arc λ'_2 , then the application of Theorem 2.7 of [15] to the quadrilateral $\hat{Q}_{0,1,2,3}$ gives that

$$0 \leq m(\hat{Q}_{0,1,2,3}) - \{m(\hat{Q}_{0,1}) + m(\hat{Q}_{2,3})\} \leq 1.28 e^{-2\pi h},$$

provided $h \geq 1$. Further, from Theorem 4 of [4] and Koebe's $\frac{1}{4}$ -theorem we have that

$$h \geq m(\hat{Q}_2) - \frac{1}{\pi} \log 4.$$

Therefore,

$$0 \leq m(\hat{Q}_{0,1,2,3}) - \{m(\hat{Q}_{0,1}) + m(\hat{Q}_{2,3})\} \leq 1.28 \times 16 e^{-2\pi m(\hat{Q}_2)}, \tag{2.7}$$

provided $m(\hat{Q}_2) \geq 1.5$. The result (2.4) follows easily from the three estimates (2.5)–(2.7), the additivity property

$$m(\hat{Q}_{0,1,2}) \geq m(\hat{Q}_{0,1}) + m(\hat{Q}_2),$$

and the fact that conformal modules are conformally invariant. \square

We consider, finally, a quadrilateral $Q := \{\Omega; z_1, z_2, z_3, z_4\}$ having the general form illustrated in Fig. 2 (where neither z_1, z_2 nor z_3, z_4 are assumed to be the end points of γ_1 or γ_2). In this case, for the statement and proof of the corresponding result, we introduce two auxiliary crosscuts γ'_1 and γ'_2 , as shown in Fig. 6. (Here, γ'_1, γ'_2 are two Jordan arcs in Ω that share the same end points with γ_1 and γ_2 respectively and, together with the crosscut l , divide Ω into four subdomains $\Omega_1, \Omega_2, \Omega_3$ and Ω_4 , so that $\bar{\Omega} = \bar{\Omega}_1 \cup \bar{\Omega}_2 \cup \bar{\Omega}_3 \cup \bar{\Omega}_4$.)

Theorem 2.3. *Let Q be the quadrilateral of Fig. 6 described above. Then, for the decomposition defined by the curved crosscut l ,*

$$0 \leq m(Q) - \{m(Q_{1,2}) + m(Q_{3,4})\} \leq 59.75 e^{-2\pi m^*}, \tag{2.8}$$

provided that $m^* := \min\{m(Q_2), m(Q_3)\} \geq 1.5$.

Proof. From [15, Theorem 2.5] we have that

$$|m(Q) - \{m(Q_{1,2,3}) + m(Q_{2,3,4}) - m(Q_{2,3})\}| \leq 2.71 e^{-\pi m(Q_{2,3})}, \tag{2.9}$$

provided $m(Q_{2,3}) \geq 3$. Also, the application of Theorem 2.2 to the quadrilaterals $Q_{1,2,3}$ and $Q_{2,3,4}$ gives, respectively, that

$$0 \leq m(Q_{1,2,3}) - \{m(Q_{1,2}) + m(Q_3)\} \leq 28.52 e^{-2\pi m^*}, \tag{2.10}$$

and

$$0 \leq m(Q_{2,3,4}) - \{m(Q_2) + m(Q_{3,4})\} \leq 28.52 e^{-2\pi m^*}, \tag{2.11}$$

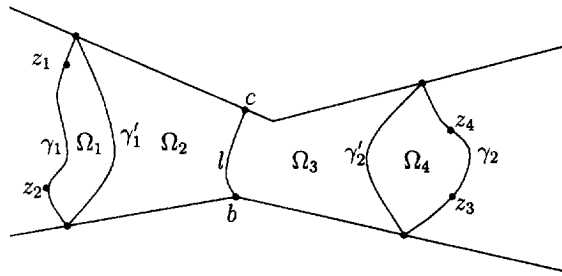


Fig. 6.

provided $m^* := \min\{m(Q_2), m(Q_3)\} \geq 1.5$. The result (2.8) follows easily from the three estimates (2.9), (2.10), (2.11) and the additivity property

$$m(Q_{2,3}) \geq m(Q_2) + m(Q_3). \quad \square$$

Remark 2.1. It is easy to show, by using continuity arguments, that the auxiliary arc γ'_2 in Fig. 5 may be taken to coincide with the boundary arc γ_2 . Similarly, the two auxiliary arcs γ'_1 and γ'_2 , in Fig. 6, may be taken to coincide with the boundary arcs γ_1 and γ_2 , respectively. This means that, in practice, it is much more convenient (and efficient) to apply the results of Theorems 2.2 and 2.3 in the following form:

(i) For the decomposition of quadrilateral $Q := \{\Omega; z_1, z_2, z_3, z_4\}$ illustrated in Fig. 7,

$$0 \leq m(Q) - \{m(Q_1) + m(Q_2)\} \leq 28.52e^{-2\pi m^*}, \tag{2.12}$$

provided that $m^* := \min\{m(Q_1), m(Q_2^*)\} \geq 1.5$, where Q_2^* is the quadrilateral

$$Q_2^* := \{\Omega_2; c, b, z_3^*, z_4^*\}.$$

(ii) For the decomposition of the quadrilateral $Q := \{\Omega; z_1, z_2, z_3, z_4\}$ illustrated in Fig. 8,

$$0 \leq m(Q) - \{m(Q_1) + m(Q_2)\} \leq 59.75e^{-2\pi m^*}, \tag{2.13}$$

provided that $m^* := \min\{m(Q_1^*), m(Q_2^*)\} \geq 1.5$, where Q_1^* and Q_2^* are the quadrilaterals

$$Q_1^* := \{\Omega_1; z_1^*, z_2^*, b, c\} \quad \text{and} \quad Q_2^* := \{\Omega_2; c, b, z_3^*, z_4^*\}.$$

Remark 2.2. Theorems 2.1–2.3 remain valid even when the domain Ω is part of a general strip-like domain (instead of an infinite polygon \mathcal{P}). In this case, however, the determination of the curved crosscuts will require the conformal map from \mathcal{S} onto the strip-like domain.

3. Examples of curved crosscuts

If the Schwarz–Christoffel map $T : \mathcal{H} \rightarrow \mathcal{P}$, of Fig. 3, is known in closed form, then the parametric equation of the associated curved crosscut l is given in exact parametric form by

$$l := \{z: z = T(e^{it}), 0 \leq t \leq 1\}. \tag{3.1}$$

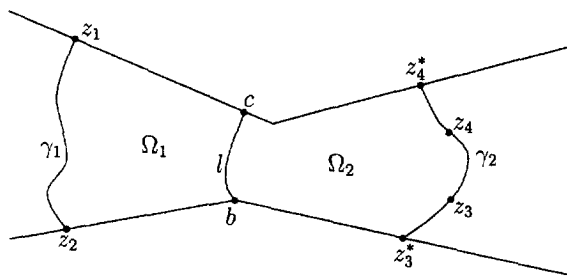


Fig. 7.

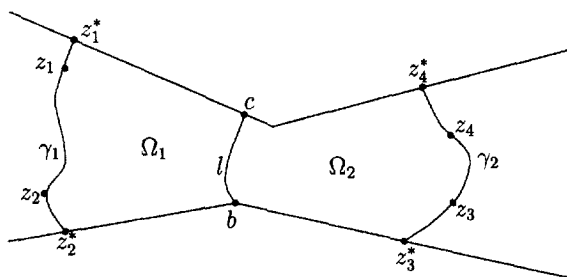


Fig. 8.

Otherwise, l can be obtained approximately by using a numerical approximation \tilde{T} to T . In particular, l can be approximated by

$$\tilde{l} := \{z: z = \tilde{T}(e^{i\pi t}), 0 \leq t \leq 1\}, \tag{3.2}$$

where \tilde{T} is an approximation to T obtained by using the Schwarz–Christoffel conformal mapping package SCPACK of Trefethen [16,18]. We illustrate the above remarks by the following examples, where in cases for which the associated Schwarz–Christoffel transformation $T: \mathcal{H} \rightarrow \mathcal{P}$ is known in closed form, we simply state the corresponding mapping function:

Example 3.1. For a quadrilateral of the form illustrated in Fig. 9 the associated Schwarz–Christoffel mapping function is

$$T(W) = \frac{i}{\kappa\pi} \log \left\{ \frac{1 + i\kappa\zeta}{1 - i\kappa\zeta} \right\} + \frac{1}{\pi} \log \left\{ \frac{1 + \zeta}{1 - \zeta} \right\}, \tag{3.3}$$

where

$$\zeta = \left\{ \frac{W - 1}{W + \kappa^2} \right\}^{1/2}$$

(see e.g. [2, p. 351] and [7, p. 157]).

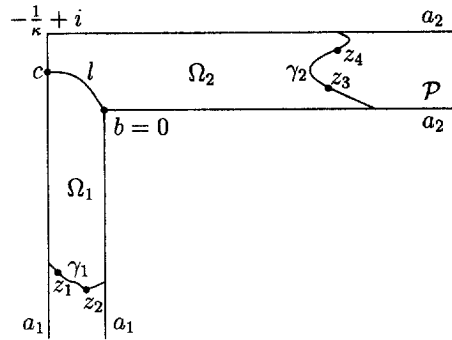


Fig. 9.

Example 3.2. For a quadrilateral of the form illustrated in Fig. 10 the associated Schwarz–Christoffel mapping function is

$$T(W) = \frac{1}{\pi} \cosh^{-1} \left\{ \frac{2\kappa^2 W - \kappa^2 - 1}{1 - \kappa^2} \right\} - \frac{\kappa}{\pi} \cosh^{-1} \left\{ \frac{(1 + \kappa^2)W - 2}{(1 - \kappa^2)W} \right\}, \tag{3.4}$$

with $0 < \kappa < 1$ (see e.g. [7, p. 161]).

Example 3.3. For a quadrilateral of the form illustrated in Fig. 11 the associated Schwarz–Christoffel mapping function is

$$T(W) = \frac{1}{\pi} \int_W^1 \frac{(1 - \zeta)^\alpha}{\zeta} d\zeta + i, \quad 0 < \alpha < 1 \tag{3.5}$$

(see e.g. [7, p. 155–156]), i.e. the crosscut l is given in parametric form by

$$z = -i \left\{ \int_0^t (1 - e^{i\pi y})^\alpha dy - 1 \right\}, \quad 0 \leq t \leq 1. \tag{3.6}$$

Thus, in this case, l must be determined by numerical quadrature.

Example 3.4. If for a quadrilateral of the form illustrated in Fig. 2 the associated transformation $T: \mathcal{H} \rightarrow \mathcal{P}$ is not known exactly, then we approximate T by

$$\tilde{T} = \tilde{T}_1 \circ T_2 \circ T_3, \tag{3.7}$$

where

- \tilde{T}_1 is the SCPACK approximation of the conformal map of the unit disc D onto \mathcal{P} .
- T_2 is the bilinear transformation mapping D onto itself so that

$$T_2(-i) = \tilde{Z}_1, \quad T_2(1) = \tilde{Z}_2 \quad \text{and} \quad T_2(i) = \tilde{Z}_3,$$

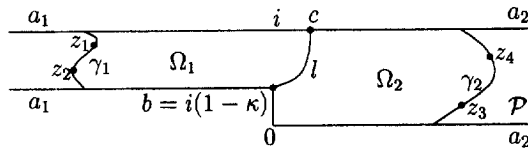


Fig. 10.

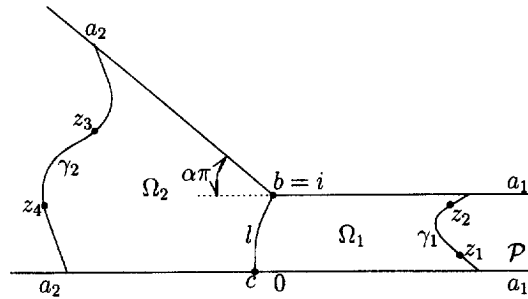


Fig. 11.

where \tilde{Z}_1 , \tilde{Z}_2 and \tilde{Z}_3 are respectively the approximate pre-images of a_1 , b and a_2 , produced by the mapping \tilde{T}_1 .

- T_3 is the bilinear transformation,

$$T_3(W) := i \frac{W - i}{W + i}, \tag{3.8}$$

mapping the upper half plane \mathcal{H} onto D so that

$$T_3(0) = -i, \quad T_3(1) = 1 \quad \text{and} \quad T_3(\infty) = i.$$

Thus, the required crosscut l is given in approximate parametric form by

$$\tilde{l} := \{z: z = \tilde{T}(e^{i\pi t}), 0 \leq t \leq 1\}, \tag{3.9}$$

where $\tilde{T} = \tilde{T}_1 \circ T_2 \circ T_3$.

In order to check the above numerical process, we consider the quadrilateral of Example 3.2, with $\kappa = 0.5$, and compare the approximate crosscut \tilde{l} , obtained by means of Eq. (3.9), with the exact crosscut given by Eq. (3.4). We do this by computing

$$\varepsilon := \max_{j=0, \dots, 100} |l(10^{-2}j) - \tilde{l}(10^{-2}j)|, \tag{3.10}$$

and find that

$$\varepsilon \leq 3.04 \times 10^{-12}.$$

This is in agreement with the SCPACK error estimate which, in this case, is 2.24×10^{-12} .

4. Numerical examples

In this section we present four numerical examples, illustrating the application of the DDM with curved crosscuts. Our objectives are as follows:

- (i) To compare the theoretical estimates for the DDM errors given by (2.3) with the actual DDM errors. We do this in Example 4.1, by considering a simple decomposition for which we can find a reliable approximation to the module of the original quadrilateral.
- (ii) To consider a case where it is possible to obtain DDM results by using straight line crosscuts and to compare these results with those obtained by using the DDM with curved crosscuts (Example 4.2).
- (iii) To present examples where the application of DDM is possible only when curved crosscuts are used and to estimate the errors of the resulting DDM approximations (Examples 4.3 and 4.4).

In our examples, if the conformal module $m(Q_j)$ of a component quadrilateral is not known exactly, then it is computed by means of the conventional method, i.e. by using the unit disc D as intermediate canonical domain (see e.g. [9, Section 3.1] and [17, Section 2]). For this purpose, we use either the Schwarz–Christoffel package SCPACK [16,18] or the double precision version of the integral equation conformal mapping package CONFPACK of Hough [6],¹ as follows:

- If Ω_j is a polygon, then the approximation to $m(Q_j)$, together with an estimate of the corresponding error, is obtained by using the subroutine RESIST of SCPACK.
- If Ω_j involves curved boundary segments, then: (a) we use CONFPACK to compute the images of the four special points of Q_j , under the conformal map $f : \Omega_j \rightarrow D$; (b) we determine the approximation to $m(Q_j)$, in the usual manner, by computing the ratio of two complete elliptic integrals of the first kind whose moduli depend only on these four images. In this case, we estimate the error in the approximation to $m(Q_j)$ by means of the following ‘rule of thumb’, which takes into account both the error in the approximation to f and the crowding of points on the unit circle (for a discussion on the crowding phenomenon and on ways for measuring the crowding of points on the unit circle, see e.g. [9, Section 3.1] and [13, Section 1]): *“If the estimate of the error in the approximation to the conformal map f is of order 10^{-d_1} and the measure of crowding is of order 10^{-d_2} , where $d_1 > d_2$, then the resulting approximation to the conformal module is correct to at least $d_1 - d_2$, decimal places”.*

Regarding the use of CONFPACK, care must be taken in order to fulfill the package’s requirement that each boundary segment of the defining domain is given by a parametric equation with non-vanishing first derivative.

Example 4.1. Consider the decomposition of the quadrilateral illustrated in Fig. 12, where the cross-cut of subdivision has the parametric form

$$l := \{z : z = T(e^{it}), 0 \leq t \leq 1\},$$

and T is the special case $\kappa = 0.5$ of the Schwarz–Christoffel mapping (3.4) in Example 3.2.

¹The double precision version of CONFPACK has only become available very recently; see <http://www.mis.coventry.ac.uk/~dthough/>.

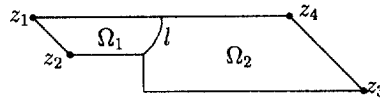


Fig. 12. The coordinates of the corners, starting from z_1 and moving in counter-clockwise order, are $(-1.5, 1.), (-1., 0.5), (0., 0.5), (0., 0.), (3., 0.), (2., 1.)$.

The approximations to the conformal modules of the component quadrilaterals Q_1 and Q_2 are obtained by using CONFPACK and are as follows:

$$m(Q_1) \approx 2.4458094834, \quad m(Q_2) \approx 2.3620709676.$$

These are expected to be correct to at least 9 decimal places, because: (a) the error estimates for the associated conformal maps onto the unit disc are 1.0×10^{-11} and 9.6×10^{-12} ; (b) the corresponding measures of crowding are 4.3×10^{-2} and 1.2×10^{-1} . Therefore, we expect that the DDM approximation to $m(Q)$ is given correct to 9 decimal places by

$$\tilde{m}(Q) := m(Q_1) + m(Q_2) = 4.807880451. \tag{4.1}$$

For the ‘actual’ value of the module of the original quadrilateral we use the subroutine RESIST of SCPACK and find that $m(Q)$ is given correct to 9 decimal places by

$$m(Q) = 4.807880808.$$

Therefore, the actual error in the DDM approximation (4.1) is

$$E := m(Q) - \tilde{m}(Q) = 3.57 \times 10^{-7}.$$

By contrast, (2.3) gives the theoretical error estimate

$$0 < m(Q) - \tilde{m}(Q) \leq 5.33e^{-2\pi \min\{m(Q_1), m(Q_2)\}} < 1.92 \times 10^{-6}$$

which, in conjunction with (4.1), leads to the following DDM prediction:

$$4.807880 < m(Q) < 4.807883.$$

Example 4.2. Consider the decomposition illustrated in Fig. 13, where the crosscuts of subdivision are all straight lines and are determined in the ‘best possible’ way by using the relevant DDM theory. (The parametric equations of the crosscuts separating Ω_1 from Ω_2 , Ω_2 from Ω_3 , Ω_3 from Ω_4 , Ω_5 from Ω_6 and Ω_7 from Ω_8 , are respectively $z = 5 + it$, $t \in [0, 1]$, $z = t + 6i$, $t \in [0, 2]$, $z = t + 15i$, $t \in [0, 1]$, $z = 6.5 + it$, $t \in [18, 19]$ and $z = t + 12.5i$, $t \in [12, 13]$.)

Regarding the components of the decomposition, the modules of the trapezoidal quadrilaterals Q_4 , Q_5 , Q_6 and Q_7 are known exactly in terms of elliptic integrals (see e.g. [12, Remark 2.4]). The modules of the other component quadrilaterals are computed by using SCPACK, in the case of Q_2 , and CONFPACK for Q_1 , Q_3 and Q_8 . The numerical results are as follows:

- To 10 decimal places,

$$m(Q_4) = 3.2793643995,$$

$$m(Q_5) = m(Q_6) = m(Q_7) = 5.7793643998.$$

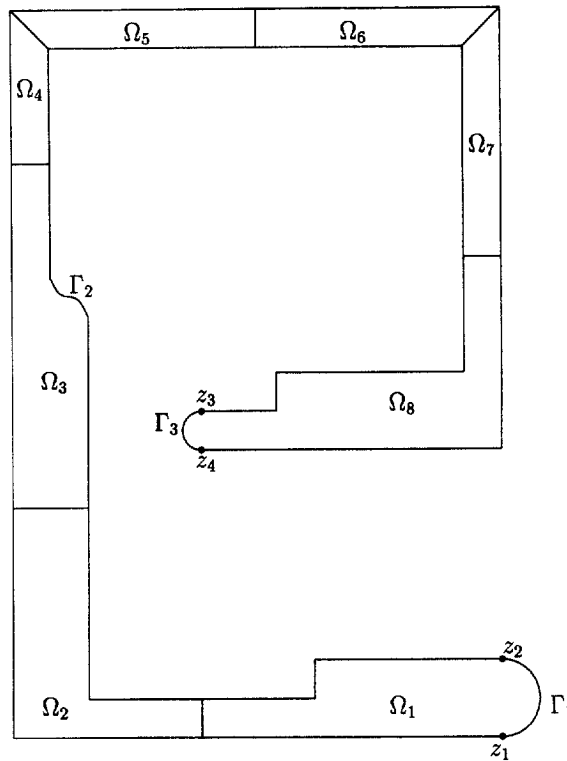


Fig. 13. The coordinates of the corners, starting from z_1 and moving in counterclockwise order, are $(13.,0.)$, $(13.,2.)$, $(8.,2.)$, $(8.,1.)$, $(2.,1.)$, $(2.,11.)$, $(1.,12.)$, $(1.,18.)$, $(12.,18.)$, $(12.,9.5)$, $(7.,9.5)$, $(7.,8.5)$, $(5.,8.5)$, $(5.,7.5)$, $(13.,7.5)$, $(13.,19)$, $(0.,19.)$, $(0.,0.)$. Γ_1 and Γ_3 are semicircles of radius 1 and 0.5 and centers at $(13.,1.)$ and $(5.,8.)$ respectively, and Γ_2 is given by the parametric equation, $z(t) = 2t^3 - 3t^2 + 2 + i(t + 11)$, $t \in [0, 1]$.

- SCPACK gives the approximation

$$m(Q_2) \approx 6.143537228,$$

which is expected to be correct to all the figures quoted.

- CONFPACK gives the approximations

$$m(Q_1) \approx 5.94518113, \quad m(Q_3) \approx 6.36125572, \quad m(Q_8) \approx 8.58892796.$$

These are expected to be correct to 6, 7 and 3 decimal places, respectively, because: (a) the error estimates for the associated conformal maps onto the unit disc are 2.8×10^{-11} , 1.1×10^{-12} and 2.3×10^{-10} ; (b) the corresponding measures of crowding are 5.9×10^{-5} , 4.8×10^{-5} and 9.8×10^{-7} .

We note that (because Q_8 is ‘long’) the crowding of points, introduced by the conformal map $\Omega_8 \rightarrow D$, affects seriously the accuracy of the CONFPACK approximation to $m(Q_8)$. As a result, we can only state with certainty that this approximation is correct to 3 decimal places.

Regarding the DDM error, the repeated application of Theorems 2.4 and 2.6 of [15] gives that

$$0 \leq m(Q) - \tilde{m}(Q) < 2.60 \times 10^{-7}. \tag{4.2}$$

However, because of the relatively poor approximation to $m(Q_8)$, we can only be certain of the first three decimal places in the resulting DDM sum

$$\tilde{m}(Q) := \sum_{j=1}^8 m(Q_j) = 47.6563596369, \tag{4.3}$$

i.e. we can only predict that $m(Q)$ is given correct to 3 decimal places by

$$m(Q) = 47.656. \tag{4.4}$$

We consider now the same quadrilateral Q but decomposed as illustrated in Fig. 14 where the straight line crosscuts are as before and the curved crosscuts l_1 and l_2 are of the form given in Examples 3.2 and 3.1, respectively, in each case with $\kappa = 0.5$.

Regarding the components of this decomposition, the quadrilaterals Q_3, Q_4, Q_5, Q_6, Q_7 and Q_8 are the same as the quadrilaterals Q_2, Q_3, Q_4, Q_5, Q_6 and Q_7 of Fig. 13. For the modules of the other four component quadrilaterals, CONFACK gives the following approximations:

$$m(Q_1) \approx 2.77862607, \quad m(Q_2) \approx 3.16655506, \tag{4.5}$$

$$m(Q_9) \approx 3.22009207, \quad m(Q_{10}) \approx 5.36881489. \tag{4.6}$$

These are expected to be correct to all the figures quoted, because: (a) the error estimates for the associated conformal maps onto the unit disc are 1.0×10^{-11} , 5.3×10^{-11} , 5.3×10^{-11} and 3.5×10^{-11} ; (b) the corresponding measures of crowding are 5.5×10^{-2} , 4.2×10^{-2} , 7.4×10^{-3} and 1.1×10^{-3} . Therefore, we expect that the DDM approximation to $m(Q)$ is given correct to 7 decimal places by

$$\tilde{m}(Q) := \sum_{j=1}^{10} m(Q_j) = 47.6563386. \tag{4.7}$$

The error in $\tilde{m}(Q)$ can be estimated by applying, as before, Theorems 2.4 and 2.6 of [15] to the various quadrilaterals associated with straight line crosscuts, and Theorem 2.1 and Estimate (2.12) of the present paper to the quadrilaterals $Q_{1,2}$ and $Q_{9,10}$ associated with the two curved crosscuts. More specifically, the application of Theorems 2.4 and 2.6 of [15] gives

$$0 \leq m(Q) - \left\{ m(Q_{1,2}) + \sum_{j=3}^8 m(Q_j) + m(Q_{9,10}) \right\} < 2.60 \times 10^{-7}, \tag{4.8}$$

while the application of Theorem 2.1 to $Q_{1,2}$ gives

$$0 \leq m(Q_{1,2}) - \{m(Q_1) + m(Q_2)\} \leq 5.33e^{-2\pi \min\{m(Q_1), m(Q_2)\}}. \tag{4.9}$$

(Remark. (4.5) and (4.9) imply that

$$5.94518113 \leq m(Q_{1,2}) \leq 5.94518127.$$

By contrast, if instead of l_1 we use a straight line crosscut joining the points $8 + i$ and 8 in Fig. 14, then from the resulting decomposition we get the approximation

$$\tilde{m}(Q_{1,2}) = 5.91598417,$$

which is correct only to 1 decimal place.)

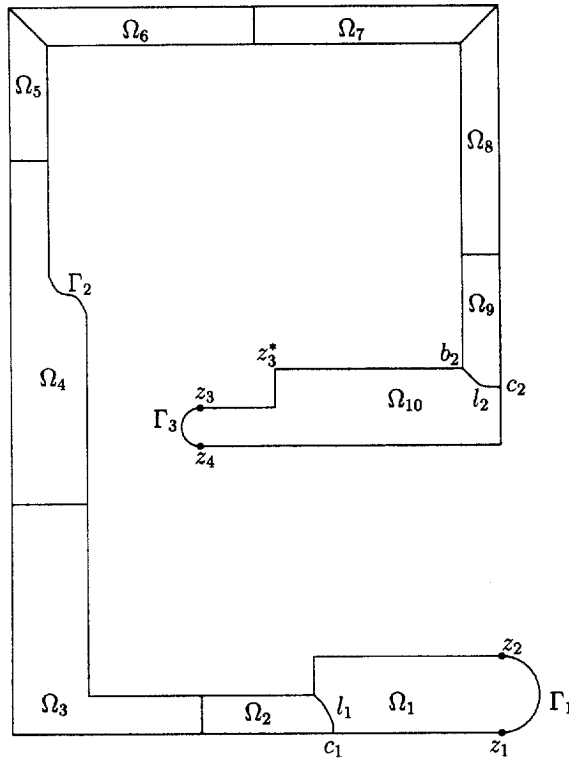


Fig. 14.

Let Q_{10}^* denote the auxiliary quadrilateral

$$Q_{10}^* := \{\Omega_{10}; c_2, b_2, z_3^*, z_4\}.$$

Then, by using CONFACK, we find that to 8 decimal places,

$$m(Q_{10}^*) = 3.00656460.$$

Therefore, since $m^* := \min\{m(Q_9), m(Q_{10}^*)\} > 1.5$, the application of (2.12) to the quadrilateral $Q_{9,10}$ gives that

$$0 \leq m(Q_{9,10}) - \{m(Q_9) + m(Q_{10})\} \leq 28.52e^{-2\pi \min\{m(Q_9), m(Q_{10}^*)\}}. \tag{4.10}$$

Hence, by combining (4.8)–(4.10), we obtain the estimate

$$0 \leq m(Q) - \tilde{m}(Q) < 5.78 \times 10^{-7}$$

which, in conjunction with Eq. (4.7), implies that

$$47.6563386 \leq m(Q) < 47.6563393. \tag{4.11}$$

Thus, by introducing the two curved crosscuts l_1 and l_2 (and using the associated DDM theory of the present paper) we are led to a much better approximation to $m(Q)$ than that obtained by using only straight line crosscuts, in the sense that we can now predict the value of $m(Q)$ correct to six decimal places.

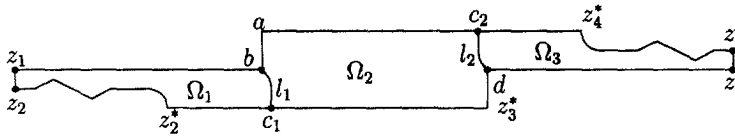


Fig. 15. The coordinates of the corners, starting from z_1 and moving in counterclockwise order, are $(-9.5, 1.)$, $(-9.5, 0.5)$, $(-9., 0.5)$, $(-8.5, 0.75)$, $(-7.5, 0.25)$, $(-7., 0.5)$, $(-6., 0.5)$, $(-5.5, 0.)$, $(3., 0.)$, $(3., 1.)$, $(9.5, 1.)$, $(9.5, 1.5)$, $(9., 1.5)$, $(8.5, 1.25)$, $(7.5, 1.75)$, $(7., 1.5)$, $(6., 1.5)$, $(5.5, 2.)$, $(-3., 2.)$, $(-3., 1.)$. The two boundary segments connecting the points $(-6., 0.5)$ to $(-5.5, 0.)$ and $(6., 1.5)$ to $(5.5, 2.)$ are quarter-circles each of radius 0.5.

Example 4.3. The quadrilateral Q illustrated in Fig. 15 does not involve sufficient symmetry for the use of the DDM with straight line crosscuts. On the other hand the direct application of CONFPACK leads to the approximation

$$m(Q) \approx 21.730. \tag{4.12}$$

This, however, cannot be relied upon because (although the CONFPACK error estimate for the associate conformal map onto the unit disc is 2.2×10^{-10}) the quadrilateral Q is ‘long’ and, as a result, the corresponding measure of crowding is 1.2×10^{-14} . Thus, because of the severe crowding, CONFPACK cannot be used directly to provide a reliable approximation to $m(Q)$. The same applies to the other general purpose conformal mapping packages, i.e. to the other packages that can deal with domains involving curved boundary segments. In fact, because of the severe crowding, the other two general purpose conformal mapping packages that are available to us, i.e. the single precision version of CONFPACK and the orthonormalisation package BKMPACK of Warby [19], fail completely in their attempt to compute $m(Q)$.

Consider now the decomposition of Q illustrated in Fig. 15, where the curved crosscuts l_1 and l_2 are both of the form given in Example 3.2, with $\kappa = 0.5$. For the modules of the three component quadrilaterals, CONFPACK gives the following approximations:

$$m(Q_1) = m(Q_3) \approx 11.31680962, \quad m(Q_2) \approx 3.1666235579.$$

These are expected to be correct to 6 and 10 decimal places respectively, because: (a) the error estimates for the conformal maps onto the unit disc are 7.3×10^{-13} , 9.7×10^{-12} ; (b) the corresponding measures of crowding are 1.5×10^{-7} , 5.5×10^{-2} . Therefore, the DDM approximation to $m(Q)$ is given, correct to 6 decimal places, by

$$\tilde{m}(Q) := m(Q_1) + m(Q_2) + m(Q_3) = 25.800243. \tag{4.13}$$

For estimating the error in $\tilde{m}(Q)$, we need to know the values of the conformal modules of the following four auxiliary quadrilaterals (see Fig. 15):

$$Q_1^* := \{\Omega_1; z_1, z_2^*, c_1, b\}, \quad Q_2^* := \{\Omega_2; a, c_1, d, c_2\},$$

$$Q_{2,3}^* := \{\Omega_{2,3}; b, c_1, z_3^*, z_4^*\}, \quad Q_3^* := \{\Omega_3; c_2, d, z_3, z_4^*\}.$$

To this end, CONFPACK gives the following approximations to $m(Q_1^*)$, $m(Q_2^*)$ and $m(Q_3^*)$:

$$m(Q_1^*) = m(Q_3^*) \approx 2.852789 \quad \text{and} \quad m(Q_2^*) \approx 3.024515,$$

which are expected to be correct to all the figures shown. Regarding the value of $m(Q_{2,3}^*)$, the comparison principle for conformal modules (see e.g. [1, p. 54]) and the rotational symmetry of Ω_2 imply that,

$$m(Q_{2,3}^*) > m(\{\Omega_2; b, c_1, z_3^*, c_2\}) = m(Q_2^*).$$

The details of the error analysis are as follows:

- Since $m^* := \min\{m(Q_1^*), m(Q_{2,3}^*)\} > 1.5$, the application of (2.13) to Q gives:

$$0 \leq m(Q) - \{m(Q_1) + m(Q_{2,3})\} \leq 59.75e^{-2\pi \min\{m(Q_1^*), m(Q_{2,3}^*)\}}.$$

- Since $m^* := \min\{m(Q_2^*), m(Q_3^*)\} > 1.5$, the application of (2.13) to $Q_{2,3}$ gives:

$$0 \leq m(Q_{2,3}) - \{m(Q_2) + m(Q_3)\} \leq 59.75e^{-2\pi \min\{m(Q_2^*), m(Q_3^*)\}}.$$

Hence, by combining the above we obtain the estimate

$$0 \leq m(Q) - \tilde{m}(Q) < 1.97 \times 10^{-6},$$

which, in conjunction with (4.13), shows that $m(Q)$ is given correct to 5 decimal places by

$$m(Q) = 25.80024. \tag{4.14}$$

This should be compared with the approximation (4.12), obtained by trying to compute $m(Q)$ directly.

Example 4.4. The quadrilateral $Q := \{\Omega; z_1, z_2, z_3, z_4\}$ illustrated in Fig. 16 does not involve sufficient symmetry for the use of the DDM with straight line crosscuts. Furthermore, the direct application of CONFPACK fails completely in this case, in the sense that (because of the severe crowding) the computer fails to recognise the images of the four special points z_1, z_2, z_3, z_4 , in the correct order on the unit circle.

Consider now the decomposition of Q illustrated in Fig. 16, where the curved crosscuts l_1 and l_3 are determined by means of SCPACK, in the way explained in Example 3.4. (The straight line crosscut l_2 is auxiliary and is needed only for the error analysis.)

The approximations for the conformal modules of the three component quadrilaterals $Q_1, Q_{2,3}$ and Q_4 are obtained by means of CONFPACK and are as follows:

$$m(Q_1) \approx 7.51137089, \quad m(Q_{2,3}) \approx 5.80190545,$$

$$m(Q_4) \approx 8.19083464.$$

These are expected to be correct to all the figures quoted, because: (a) the error estimates for the associated conformal maps onto the unit disc are 4.3×10^{-13} , 2.0×10^{-12} , 1.9×10^{-13} ; (b) the corresponding measures of crowding are 1.2×10^{-5} , 2.3×10^{-4} , 3.5×10^{-5} . Therefore, the DDM approximation to $m(Q)$ is given, correct to 8 decimal places, by

$$\tilde{m}(Q) := m(Q_1) + m(Q_{2,3}) + m(Q_4) = 21.50411098. \tag{4.15}$$

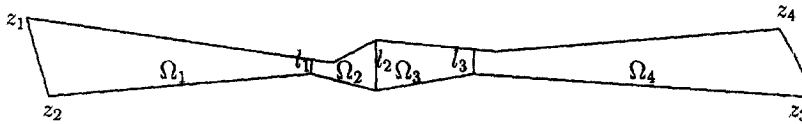


Fig. 16. The coordinates of the corners, starting from z_1 and moving in counterclockwise order, are $(-26., 5.), (-24., -2.), (0., 0.), (6., -1.5), (15., 0.), (45., -2.), (43., 4.), (17., 2.), (6., 3.), (2., 1.)$. The curved segment connecting the points z_3 and z_4 is given by the parametric equation, $z(t) = -4t^3 + 2t + 45 + (4t^3 + 2t^2 - 2)i$, $t \in [0, 1]$.

For estimating the error in $\tilde{m}(Q)$, we need to know the values of the conformal modules of the two auxiliary quadrilaterals Q_2 and Q_3 . To this end, the use of CONFPACK gives the approximations

$$m(Q_2) \approx 2.96855956 \quad \text{and} \quad m(Q_3) \approx 2.82678466,$$

which are expected to be correct to all the figures shown.

The details of the error analysis are as follows:

- Since $m^* := \min\{m(Q_1), m(Q_2)\} > 1.5$, the application of Theorem 2.2 to the decomposition of Q , defined by l_1 , gives:

$$0 \leq m(Q) - \{m(Q_1) + m(Q_{2,3,4})\} \leq 28.52e^{-2\pi \min\{m(Q_1), m(Q_2)\}}.$$

- Since $m^* := \min\{m(Q_3), m(Q_4)\} > 1.5$, the application of Theorem 2.2 to the decomposition of $Q_{2,3,4}$, defined by l_3 , gives:

$$0 \leq m(Q_{2,3,4}) - \{m(Q_{2,3}) + m(Q_4)\} \leq 28.52e^{-2\pi \min\{m(Q_3), m(Q_4)\}}.$$

Hence, by combining the above we obtain

$$0 \leq m(Q) - \tilde{m}(Q) \leq 7.8 \times 10^{-7},$$

which, in conjunction with (4.15), gives that

$$21.5041109 \leq m(Q) \leq 21.5041118.$$

References

- [1] L.V. Ahlfors, *Conformal Invariants: Topics in Geometric Function Theory*, McGraw-Hill, New York, 1973.
- [2] R.V. Churchill, J.W. Brown, *Complex Variables and Applications*, 5th ed., McGraw-Hill, New York, 1990.
- [3] D. Gaier, W.K. Hayman, Moduli of long quadrilaterals and thick ring domains, *Rend. Mat. Appl.* 10 (1990) 809–834.
- [4] D. Gaier, W.K. Hayman, On the computation of modules of long quadrilaterals, *Constr. Approx.* 7 (1991) 453–467.
- [5] P. Henrici, *Applied and Computational Complex Analysis*, vol. III, Wiley, New York, 1986.
- [6] D.M. Hough, *User's Guide to CONFPACK*, IPS Research Report 90-11, ETH-Zentrum, CH-8092 Zurich, Switzerland, 1990.
- [7] H. Kober, *Dictionary of Conformal Representations*, Dover, New York, 1957.
- [8] R. Laugesen, Conformal mapping of long quadrilaterals and thick doubly connected domains, *Constr. Approx.* 10 (1994) 523–554.
- [9] N. Papamichael, Numerical conformal mapping onto a rectangle with applications to the solution of Laplacian problems, *J. Comput. Appl. Math.* 28 (1989) 63–83.
- [10] N. Papamichael, N.S. Stylianopoulos, On the numerical performance of a domain decomposition method for conformal mapping, in: St. Ruscheweyh, E.B. Saff, L.C. Salinas, R.S. Varga (Eds.), *Computational Methods and Function Theory 1989*, Lecture Notes in Math., vol. 1435, Springer, Berlin, 1990, pp. 155–169.

- [11] N. Papamichael, N.S. Stylianopoulos, A domain decomposition method for conformal mapping onto a rectangle, *Constr. Approx.* 7 (1991) 349–379.
- [12] N. Papamichael, N.S. Stylianopoulos, A domain decomposition method for approximating the conformal modules of long quadrilaterals, *Numer. Math.* 62 (1992) 213–234.
- [13] N. Papamichael, N.S. Stylianopoulos, On the theory and application of a domain decomposition method for computing conformal modules, *J. Comput. Appl. Math.* 50 (1994) 33–50.
- [14] N. Papamichael, N.S. Stylianopoulos, Domain decomposition for conformal maps, in: R.M. Ali, St. Ruscheweyh, E.B. Saff (Eds.), *Computational Methods and Function Theory 1994*, Ser. Approx. Decompos., vol. 5, World Scientific, River Edge, NJ, 1995, pp. 267–291.
- [15] N. Papamichael, N.S. Stylianopoulos, The asymptotic behavior of conformal modules of quadrilaterals with applications to the estimation of resistance values, *Constr. Approx.* 15 (1999) 109–134.
- [16] L.N. Trefethen, Numerical computation of the Schwarz–Christoffel transformation, *SIAM J. Sci. Statist. Comput.* 1 (1980) 82–102.
- [17] L.N. Trefethen, Analysis and design of polygonal resistors by conformal mapping, *J. Appl. Math. Phys.* 35 (1984) 692–704.
- [18] L.N. Trefethen, *SCPACK User’s Guide*, Numerical Analysis Report 89-2, Dept. of Maths, MIT, Cambridge, MA, 1989.
- [19] M.K. Warby, *BKMPACK User’s Guide*, Technical Report, Dept. of Maths and Stats, Brunel Univ., Uxbridge, UK, 1992.